Uplift Capacity of Light-Frame Rafter to Top Plates Connections Applied with Elastomeric Construction Adhesives

Bilal Alhawamdeh, S.M.ASCE[1]; and Xiaoyun Shao, P.E., M.ASCE[2]

Abstract: The effects of the application of elastomeric construction adhesives on the wind uplift resistance of light-frame wood connections were investigated and are presented in this paper. Previous research has revealed that proper roof-to-wall connections play a critical role in mitigating structural damage during severe winds by providing a continuous load transfer path from the roof down to the foundation. Monotonic uplift tests of 30 rafter-to-top-plates connections of six configurations were conducted. Two specimen groups, standard ring shank nails alone and strengthened with hurricane ties, were constructed with and without elastomeric adhesive application, and their wind uplift resistances were compared to explore the effectiveness of the two adhesives (i.e., polyurethane and polyether) when applied to the roof connections. Experimental results show that the addition of adhesives allowed both groups to resist higher uplift loads (approximately 200%–460%) and dissipate considerably more energy (approximately 200%–750%). Replacing hurricane ties with the adhesives approximately doubles the uplift capacity but reduces the energy dissipation by nearly half owing to reduced deformation capacity. Failure modes were also examined to provide reasonable explanations for the observed performance of the connections. **DOI: 10.1061/(ASCE)MT.1943-5533.0003152.**

Introduction

Light-frame wood construction accounts for approximately 90% of the residential buildings in the US. These buildings are considered vulnerable to damage caused by severe wind events such as hurricanes and tornados (Ellingwood et al. 2004). The 2017 hurricane season was unprecedented by many observers, and it is becoming the new average. The intensity of hurricanes Irma, Harvey, and Maria caused widespread devastation, resulting in 3,259 deaths and an estimated $265.0 billion in losses, including significant damage to wood buildings (NOAA National Centers for Environmental Information 2017). Apparently, the lack of performance of light-frame constructions is a primary reason for those economic losses. Therefore, there is a strong necessity to develop and verify new and affordable materials and construction methods to mitigate the dangerous effects on structures due to extreme wind events. In addition, building codes should consider adopting these improved and affordable methods to ensure safety for building occupants.

Investigations conducted by the Federal Emergency Management Agency (FEMA) showed that failed or missed roof connections would reroute the loads through unintended load paths, often resulting in building damage or collapse [FEMA 2012; FEMA 548 (FEMA 2006)]. For light-frame wood buildings, roof failures generally begin at the connections, because of their inadequacy to resist and transfer loads. Among the various connections in the roof system, the rafter-to-top-plates connection is critical in the continuous load path. With the acknowledgment that this roof connection is a vulnerable link in the load path during extreme wind events and that the rafter connection using toenailing only is not satisfactory, increasing emphasis has been placed on the use of specialized hardware for wood framing connections in high-wind regions to ensure a continuous load path (e.g., FEMA 2010; IBHS 2019).

Many researchers (Cheng 2004; Conner et al. 1987; Edmonson et al. 2012; Reed et al. 1997; Rosowsky et al. 1998; Satheeskumar et al. 2016; Shanmugam et al. 2011) have sought to increase the uplift wind capacity for roof connections. The use of traditional metal connectors, such as straps, ties, and clips connected with nails, screws, bolts, and extra nailing, has resulted in significant increases in uplift capacity compared with standard nailing connections and thus met code for wind loads in high-wind regions. However, these mechanical fasteners have several drawbacks. They are intrusive connections that can create a path for a water leak by penetrating holes, weaken connecting wood members by intense penetration of closely spaced nails or screws, and deteriorate at a high rate in severe environments such as coastal areas (Canbek et al. 2011). Furthermore, they are susceptible to wind-induced fatigue damage because they concentrate stresses at a few localized spots in the contact areas of nails and screws in connecting members (Henderson et al. 2009) and are considerably affected by construction defects. For instance, if two nails required by the manufacturer for a metal framing anchor are missed, the uplift capacity would be reduced by almost half (Satheeskumar et al. 2016).

Historically, these issues related to mechanical fasteners prompted many researchers to explore viable alternatives to strengthen wood frame buildings. There was an interest in investigating adhesive materials to reduce the number of roof failures due to uplift load impact. Unlike mechanical fasteners, adhesives do not damage substrates and do not concentrate stress at localized spots, thus increasing uplift resistance by distributing the load to a larger contact area. In addition, the application of adhesives has gained attention for its perceivable better bonding performance

[1]Doctoral Student, Dept. of Civil and Construction Engineering, Western Michigan Univ., Kalamazoo, MI 49008. ORCID: https://orcid.org/0000-0002-0422-2933. Email: bellalmohamad@yahoo.com

[2]Associate Professor, Dept. of Civil and Construction Engineering, Western Michigan Univ., Kalamazoo, MI 49008 (corresponding author). Email: xiaoyun.shao@wmich.edu

Note. This manuscript was submitted on January 14, 2019; approved on October 11, 2019; published online on February 24, 2020. Discussion period open until July 24, 2020; separate discussions must be submitted for individual papers. This paper is part of the ***Journal of Materials in Civil Engineering***, © ASCE, ISSN 0899-1561.

over continuous interfaces and increased stiffness and durability. The ability of an adhesive to be cured in an irreversible process also helps provide high integration to connection components (Loushin 2012). The effects of epoxy, acrylic foam, and coating adhesive materials on wood frame roof connections have been investigated, considering both new construction and retrofit cases (Alldredge et al. 2012; Conner et al. 1987; Datin et al. 2011; Jacobs 2003; Reed et al. 1997; Turner et al. 2009). It was observed from these researches that increased uplift resistance was generally obtained compared with traditional nails, and some adhesive materials also provided prevention of multiple threats such as moisture migration and air leaks. However, most of the research that applied functional adhesive materials to connections primarily investigated their capacity and behavior, with less attention to cost-effectiveness, applicability, and efficiency. The proper application of coating and foaming materials is very dependent on equipment and applicator. The spray equipment that ensures optimum mixing and the raw materials are rather costly. Some adhesives have shown only a slight increase in load capacity compared with traditional nailing, because of their lower strength and improper application. These deficiencies in previous studies might be overcome through the selection of newly developed adhesives with optimum mechanical and chemical properties, and through proper application that is extended to the full contact area between the connection members to ensure better load transfer.

Therefore, an affordable, efficient, and nonintrusive roof-to-wall connection for light-frame wood construction using elastomeric adhesives is proposed. Specifically, polyurethane and polyether adhesives were adopted and applied to the rafter-to-top-plates connections. To evaluate the uplift capacity of the proposed roof connection using the elastomeric adhesives, and to explore the potential of these two adhesives for broader application in new construction, various connection specimens were built and tested under monotonic uplift loading. Uplift performance was experimentally evaluated, including force–displacement behavior, failure mode, uplift load capacity, and energy dissipation. Material properties, construction procedures, test setup, and experimental results are discussed in detail in the following sections.

Uplift Tests

Materials

Construction adhesives usually contain several elastomeric ingredients that account for a total of 30%–50% of the composition by weight. These elastomer ingredients include resins (chemical compounds used in formulating adhesives to increase the adhesion), rubber, filler, and solvents (Tse 1989). The different proportions of these ingredients make it possible to create either a contact cement with low viscosity or an extrudable mastic with a more viscous character. Cement materials are usually applied through spraying or spreading, whereas mastics are extruded through a nozzle (Forest Products Laboratory 1978). Historically, mastic adhesives have been more prevalent in wood construction because of their viscosity and gap-filling capabilities. They are used to bond plywood decking to floor joists in bonded floor systems and bond wall panels and drywalls to studs (Frihart and Beecher 2016). Because of their stiffness, mastics provide advantages in nail-bonding floor systems, resulting in savings in construction costs. In the installation of vertical drywalls or walls, a minimum of nails is required because of the wet tack inherent in mastics (Gillespie and River 1972). In this study, we adopted commercially available mastic adhesives, namely polyurethane and polyether. These adhesives are synthetic, thermosetting, moisture curing, and solvent free. They can be converted by chemical reaction with moisture at the time of use to a tough state. This reaction is not reversible once the cure is achieved.

Table 1 lists all the materials used to construct the test specimens in this study. Douglas fir wood of Grade 2 or better was used for the test specimens because of its high strength and uniform properties compared with softwoods such as southern yellow pine (Forest Products Laboratory 1952). Ring-shank nails were chosen in constructing test specimens according to the ASTM F1667 Standard Specification for Driven Fasteners (ASTM 2017a) for their superior performance over smooth shank nails in minimizing damages in high-wind areas (Rammer et al. 2001). The wood fills the crevice of the rings, providing friction to help prevent the nail from backing out over time. The Simpson Strong-Tie, Type H2.5A (Simpson Strong Ties 2019), was selected to meet the strength requirements specified in ASTM F1667, and two types of nails (8d and 6d nails) were used to fasten the tie to the rafter and the top plate, respectively. The shear strength of the two adhesives used in this study was determined according to the standard lap shear tests specified in ASTM D2339 (ASTM 2017b). The polyurethane had approximately 70% more strength than the polyether.

A rough cost estimation, carried out based primarily on the material cost, showed that the costs of roof connections using adhesives and hurricane ties are comparable. One cartridge of the adhesive product used in this study can cover seven connections for about $7, which means $1/connection. The connection using hurricane ties also costs approximately $1/connection, including about $0.60 for the tie and the remaining cost for the nails.

Test Specimen

A total of 30 rafter-to-top-plate specimens representing six configurations and five specimens of each configuration were fabricated and tested under monotonic loading. The dimensions of the rafters

Table 1. Construction materials properties in test connections

Material	Description	Dimensions/properties
Wood rafter and top plates	Douglas fir No. 2	2 by 8
Fasteners		
Ring shank nails	Paper tap offset round head	2.9 × 60.3 mm (0.113 × 2 − 3/8 in.)
Hurricane tie	Simpson H 2.5A	152 × 0.35 mm (6 × 1 − 3/8 in.)
Nails to top plates (5)	Hurricane tie nails	3.3 × 63.5 mm (0.131 × 2.5 in.)
Nails to rafter (5)	Hurricane tie nails	3.3 × 38.1 mm (0.131 × 1.5 in.)
Adhesive		
Polyurethane		Shear strength: 4.94 MPa (717 psi) Service temperature: −17.8°C (0°F) to −71.1°C (160°F)
Polyether		Shear strength: 2.88 MPa (418 psi) Service temperature: −23.3°C (−40°F) to −93.3°C (200°F)

J. Mater. Civ. Eng., 2020, 32(5): 04020078

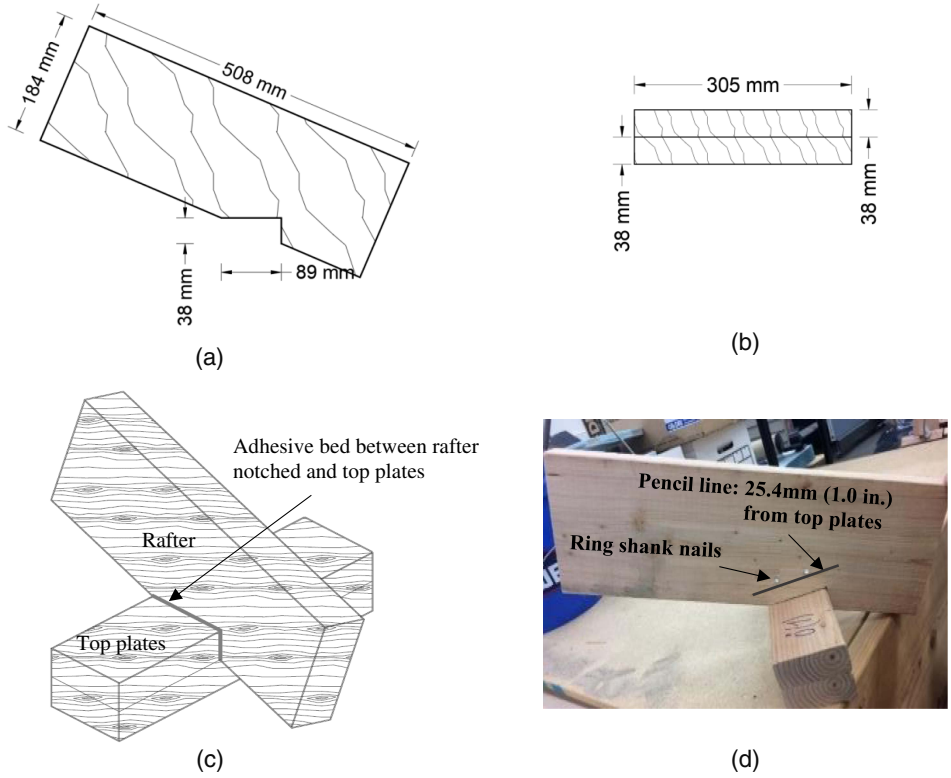

Fig. 1. Test specimen: (a) rafter dimension; (b) top plates dimension; (c) 3D view; and (d) toenailed connection construction.

and top plates used in constructing the 30 connection specimens are shown in Figs. 1(a and b), and Fig. 1(c) shows a 3-dimensional (3D) illustration of the test specimen.

Nailed connections with and without hurricane ties were the reference specimens. Polyurethane and polyether adhesives were applied to these two types of connections between the top plates and the rafter, covering the entire cross-section of the notch and resulting in four more configurations. All the test specimens and their respective configuration indices are summarized in Table 2. Note that the connections with and without hurricane ties are referred to as tied and untied configurations hereafter.

A licensed carpenter was contracted to prepare the 30 rafters with a birdsmouth notch to accept the top plate. Double top plates were first nailed together using four or more ring shank nails and then fastened to the rafter using three more ring shank nails driven by a pneumatic nail gun approximately 45° from the horizontal. A pencil line parallel to the notch's edge at a vertical distance of 25.4 mm (1.0 in.) was drawn [Fig. 1(d)] to guide the nail placement so that the same penetration length of the nails into the specimens would be obtained. Adhesives were applied approximately 3 mm (0.118 in.) thick and cured for at least 7 days as required by the manufacturer. For the tied configurations, the hurricane ties were fastened between the top plates and the rafter by traditional hand-driven nails; the nailing schedule and dimensions are provided in Table 1. Representative testing specimen configurations are shown in Fig. 2.

Test Setup

A rigid steel fixture was designed and fabricated to hold the test specimen in the loading frame and transfer the uplift loads (Fig. 3). An MTS 318.10 testing machine with a capacity of 100 kN (22.4 kips) was used to apply the predefined monotonic displacement-controlled loading protocol at a rate of 2.54 mm/min (0.1 in./min) according to the ASTM D1761 standard (ASTM 2012). Whereas welding points rigidly fixed the lower part of the steel fixture, the upper part could swivel freely as a universal joint to minimize the undesirable effect of loading misalignment. Uplift loading effects were introduced to the test specimens by imposing a displacement from the bottom to the test specimen through the lower steel fixture while the upper steel fixture was kept in place (Fig. 3). Load responses were collected using the MTS embedded sensors at a rate of 100 Hz, and photos were taken to record the failure behavior of the test specimens at various loading stages.

Table 2. Six connection configurations and their indices

Index	Group	Description	No. of specimens
N	Untied (without hurricane ties)	Nails only	Five of each configuration; total 30 specimens
N-PE		Nails + polyether	
N-PU		Nails + polyurethane	
N-T	Tied (with hurricane ties)	nails + tie	
N-T-PE		Nails + tie + polyether	
N-T-PU		Nails + tie + polyurethane	

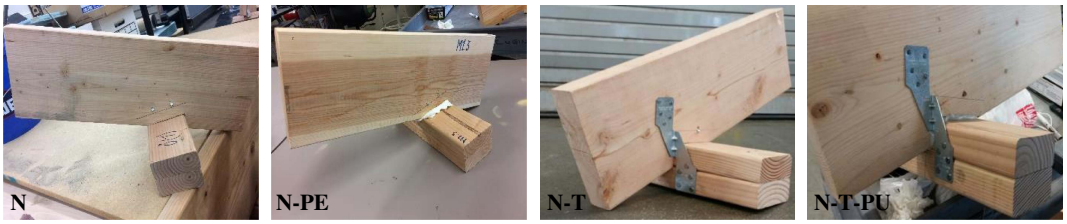

Fig. 2. Test specimen configurations: (a) N; (b) N-PE; (c) N-T; and (d) N-T-PU.

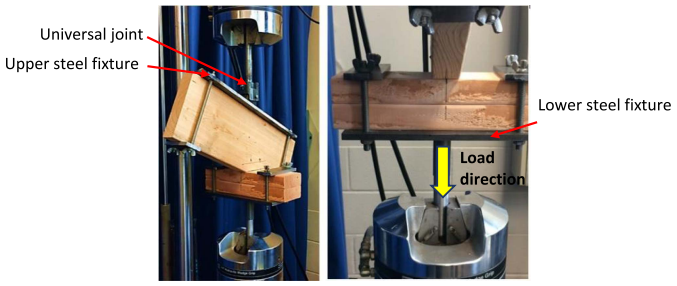

Fig. 3. Test setup.

Results

To evaluate the performance of the proposed roof connection and quantify the effects of using the elastomeric adhesives on the uplift resistances, a total of 30 specimens of six configurations and five specimens of each configuration were tested, and the results were evaluated.

The force–displacement curve of each specimen was obtained first using the measured data, based on which an average curve was generated for each configuration using the computed average force at a specified displacement versus that displacement value. The characteristic parameters of the six configurations were then determined using their respective average curve based on the definitions illustrated in Fig. 4 and explained next.

The maximum load, $P_{\max}$, is defined as the peak load measured from the entire curve. The failure load, $P_{failure}$, is the last peak load before the complete failure (Fig. 4). In this paper, $P_{failure}$ and its corresponding displacement, $\Delta_{failure}$, are used to represent the load capacity and the deformation capacity of the connections,

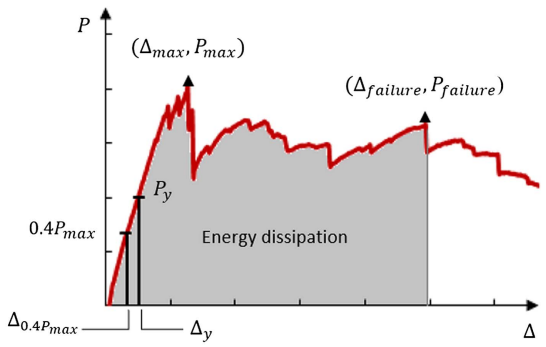

Fig. 4. Definition of the characteristic parameters using force–displacement curves.

respectively. The areas under the curve before the failure load give a measure of the amount of energy dissipation of the connection up to failure (Dias 2015). In addition, the initial stiffness and the ductility ratio were determined for each configuration according to the illustration in Fig. 4. Whereas the initial stiffness was determined by fitting a straight line through the initial linear portion of the force–displacement curve up to the load corresponding to 40% of the $P_{\max}$ (ASTM 2018), the ductility ratio of the connection was the ratio of $\Delta_{failure}$ over the displacement at the proportional yield limit, Δ_y (Muñoz et al. 2008).

Force–Displacement Curves

Fig. 5 shows individual force–displacement curves of the five specimens and the average curve of the six configurations. A detailed discussion of these curves is provided next for the reference configurations (N and N-T) and the two groups of tied and untied configurations.

Reference Configuration

The force–displacement curves of the N and N-T configurations, as shown in Figs. 5(a and d), respectively, were used as the reference for the two specimen groups and were compared with the curves of their counterparts where the adhesives were applied. The N and N-T curves can be described as curvilinear, with a relatively straight-line segment representing the initial linear elastic behavior under small loads, and then a flatter line segment indicating the plastic response until failure. After the N-T specimens reached their $P_{\max}$ of around 3.9 kN (876.8 lb), the average strength reduction in the load was approximately 14% until failure occurred. In contrast, N specimens typically failed with a $P_{\max}$ of 1.9 kN (427.1 lb), and the displacement at failure was much lower than that of the N-T specimen.

The LRFD design capacities of these two reference configurations were computed based on the National Design Specification (NDS) (American Wood Council 2018) and the data from the manufacturer's catalog (Simpson Strong Ties 2019). The calculation procedure is demonstrated in Table 3. The design value of the N configuration, W'_N, was determined to be 0.94 kN (212 lb). Compared with the test result of $P_{\max} = 1.9$ kN (340 lb), the safety factor in the NDS is approximately 2. The design value of the N-T configuration, W'_{N-T}, was estimated by adding the design capacities of the N configuration W'_N to the hurricane tie W'_H, which resulted in 3.8 kN (872 lb). However, the higher load capacities of the N-T specimens would be expected if the nails used in the construction (Table 1) were the same as those specified in the catalog (see footnote in Table 3). Therefore, compared with the test result of 3.9 kN (877 lb), the safety factor for the N-T configuration is slightly higher than 1, based on the catalog data and the NDS method.

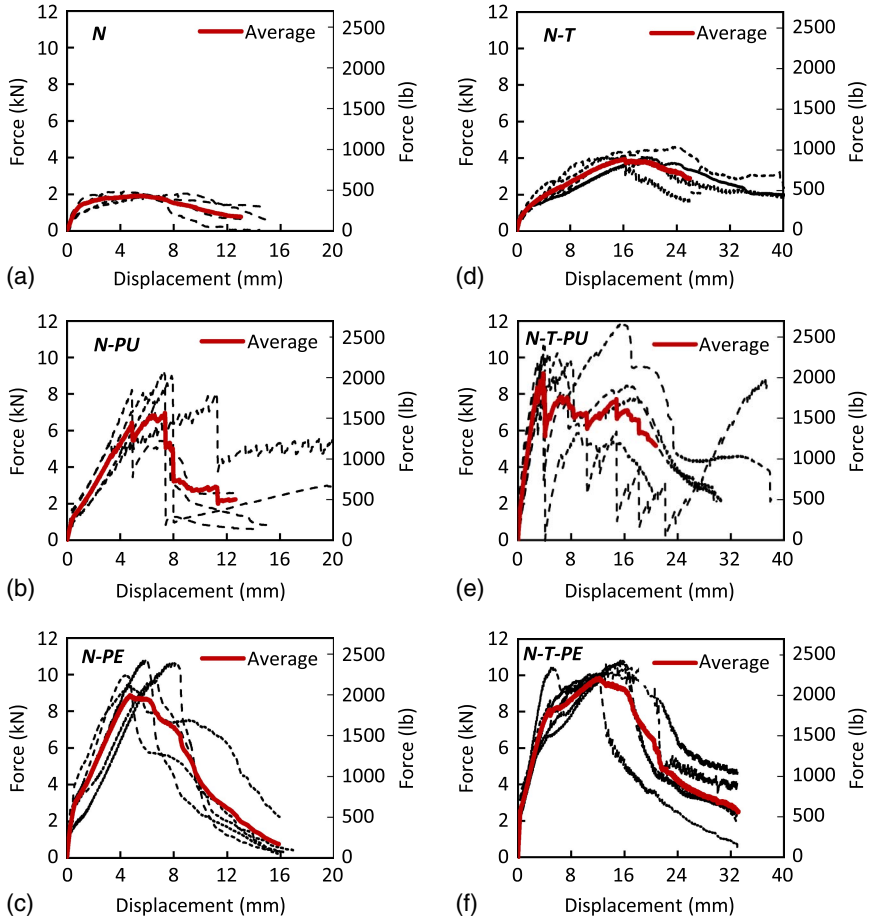

Fig. 5. Force–displacement curves of the six configurations: (a) N; (b) N-PU; (c) N-PE; (d) N-T; (e) N-T-PU; and (f) N-T-PE. (Conversion: 1 in. = 25.4 mm).

Table 3. LRFD design capacities for N and N-T configurations

Parameter	Definition	Value
W_H	LRFD design capacity of hurricane tie H 2.5A	2.9 kN (660 lb)[a]
ϕ	Resistance factor	0.65
G	Specific gravity of the wood	0.5 for Douglas fir
D	Nail shank diameter	2.9 mm (0.113 in.)
L	Nail total penetration length	73.2 mm (2.88 in.)
C_{tn}	Toenail factor	0.67
K_f	Format conversion factor	3.32
C_M, C_t, C_{eg},	Wet service, temperature, grain, and time effect factors	1
W'_N	$\phi(1{,}800G^2D)LC_{tn}K_fC_M^2C_tC_{eg}\lambda$	0.94 kN (212 lb)
W'_{N-T}	$W'_N + W'_H$	3.8 kN (872 lb)

[a]Based on being fastened using five 3.3 × 63.5-mm (0.131 × 2.5-in.) nails to both top plates and rafter (Simpson Strong Ties 2019).

Untied Configuration

The force–displacement curves of untied configurations with polyether and polyurethane adhesives are shown in Figs. 5(b and c), respectively. The force–displacement behavior of the N-PU specimens showed several drops in the load owing to the wood failure observed during the test. Its corresponding average force–displacement curve appears to be erratic, with a steep load reduction of 200% after its P_{max}, which indicates that the N-PU specimens failed in a brittle manner [Fig. 5(b)].

In contrast, the N-PE configuration showed a P_{max} of 8.9 kN (2,000 lb) without noticeable sudden load drop [Fig. 5(c)]. However, once the specimen reached its P_{max}, the load started to reduce gradually until the two parts of the connection (i.e., rafter and double top plates) were completely separated. This configuration failed in a relatively ductile manner under visible deformations beyond the yield limit, with no sudden load reduction.

Tied Configuration

The force–displacement curves of the tied configurations with polyether and polyurethane adhesives are shown in Figs. 5(e and f), respectively. Unlike the N-T-PU specimens, whose peak loads exclusively occurred at the apexes of the force–displacement curves [Fig. 5(e)] with an average P_{max} of 9.1 kN (2,046 lb) and a corresponding displacement of 3.8 mm (0.15 in.), the N-T-PE specimens showed larger plateaus, where they maintained to carry the loads close to the P_{max} over a wide displacement range. The average P_{max} was 9.9 kN (2,225 lb), with a corresponding displacement of about 12.2 mm (0.48 in.), as shown in Fig. 5(f).

Average Force–Displacement Curves

For easy comparison of all six configurations, the average force–displacement curves are plotted in the same figure (Fig. 6).

The average curve of the configurations of the polyurethane adhesive (i.e., N-PU and N-T-PU) shows that the connection experienced multiple drops in the load and then increased. This behavior is related to the shear strength of the polyurethane, which is 70% higher than that of the polyether (Table 1), which provides higher

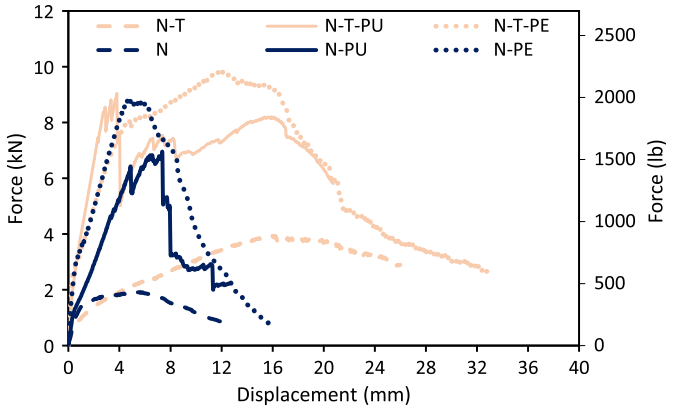

Fig. 6. Average force–displacement curves. (Conversion: 1 in. = 25.4 mm).

bond strength that exceeds the wood strength. Once the wood fiber breaks, the load capacity suddenly drops. Meanwhile, the remaining intact wood or the hurricane tie begins to take more load, providing additional strength to the connection. The failure modes of these configurations, discussed in the next section, provide further explanation for the load drops in these curves (Fig. 6).

In general, adding adhesives significantly increased the load capacities and reduced the deformation under the same level of load compared with the reference specimens, as can be seen in Fig. 6. Taking the tied group as an example, under the load level of 2 kN (455 lb), the deformation of the connections with adhesives (i.e., N-T-PE and N-T-PU) is approximately 1/10th of the deformation of the N-T configuration. Similar observations can be made about the untied group. This reduced deformation induced by the application of adhesives is desirable in light-frame wood construction, where smaller openings lead to less water and air intrusions, and thus reduce damage loss.

On the other hand, the addition of hurricane ties allowed an increase in both load capacities and deformation capacities compared with the untied configurations. Increased deformations under higher loads for the tied group indicates that a significant amount of energy dissipation was achieved. A quantitative analysis of the characteristic parameters determined based on these average curves is provided later to further facilitate the comparison.

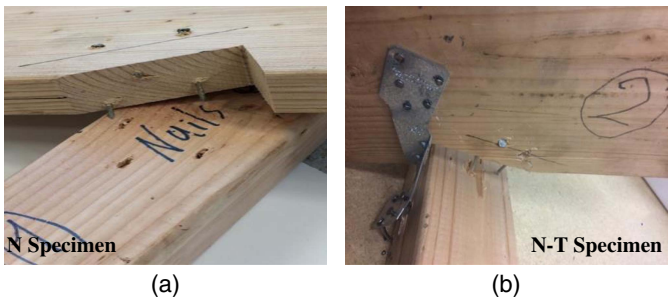

Fig. 7. Failure modes of nails: (a) pulling out from top plate; and (b) pulling out from rafter.

Failure Modes

The failure behavior of the tested specimens is presented to provide interpretations of the specimens' capacities and identify the primary impacts. The typical failure mode of the N and N-T configurations is nails pulling out, from either the top plate or the rafter [Figs. 7(a and b)]. For the N-T specimens, the hurricane ties usually experienced minimum bend at failure. No visible deformation in the ties means that the connection construction did not fully engage their strengths, as shown in Fig. 7(b).

For the connections with adhesives, the connection experienced either cohesive failure or wood failure, depending on the relative strength of the wood and the adhesive. When the adhesion to the substrate provided by the adhesive was stronger than the adhesive shear strength itself but weaker than the wood strength, cohesive failure would occur, which is the failure that occurred in the bulk layer of the adhesive. This type of failure was observed in the configurations with polyether, as shown in Fig. 8(a).

On the other hand, when both the adhesion to the wood substrate and the adhesive strength within itself are stronger than the wood strength, the failure would occur in the wood fiber in a brittle manner. Such failure would result in either a rafter splitting or a top plate tearing [Figs. 8(b and c)], and it is predominant in the specimens using the polyurethane adhesive because of its higher bonding and shear strength compared with the polyether (Table 1). The load capacity of the configurations using polyurethane, therefore, became a function of the tensile strength of the wood.

Characteristic Parameters

According to the definitions of the characteristic parameters presented earlier, load and deformation capacities, energy dissipation, ductility ratio, and initial stiffness of each configuration were determined and are summarized in Table 4. In addition, the coefficients of variation (COV) of the load capacities are included as a consistency index of each configuration. Note that the P_{max} coincided with $P_{failure}$ for all configurations except N-T-PU (Fig. 6). Therefore, $\Delta_{failure}$ is equal to Δ_{max} for all configurations except N-T-PU as well, whose $\Delta_{failure}$ is relatively larger, as listed in the table.

Fig. 8. Failure modes in configurations using adhesives: (a) cohesive failure in N-PE; (b) rafter splitting in N-PU; and (c) top plate fibers tearing in N-PU.

Table 4. Characteristic parameters of the six specimen configurations

Conf. index	Load capacity ($P_{failure}$), kN (lb)	COV load	Deformation capacity ($\Delta_{failure}$), mm (in.)	Energy dissipation, kN · mm (lbs · in.)	Ductility ratio[a]	Initial stiffness[b], kN/mm (kips/in.)
N	1.9 (430)	0.07	5.1 (0.2)	4.1 (36)	4.6	0.6 (3.4)
N-PU	7.0 (1,574)	0.29	7.4 (0.29)	31.1 (275)	1.5	1.6 (8.6)
N-PE	8.9 (2,000)	0.11	4.7 (0.19)	25.8 (228)	9.0	3.2 (18.3)
N-T	3.9 (877)	0.08	16.2 (0.64)	42.0 (372)	4.5	0.7 (4.0)
N-T-PU	8.1 (1,820)	0.17	14.8 (0.58)	98.9 (875)	3.7	3.8 (21.7)
N-T-PE	9.9 (2,226)	0.09	12.2 (0.48)	91.4 (809)	12.1	2.8 (16.0)

[a]Ductility ratio $= \frac{\Delta_{failure}}{\Delta_{yield}}$.

[b]Initial stiffness $= \frac{0.4P_{max}}{\Delta_{0.4P_{max}}}$.

As can be seen from the load capacity results, the addition of polyurethane and polyether allowed both the untied and tied configurations to withstand higher load capacity, leading to dissipation of a considerable amount of energy compared with their counterparts (i.e., those specimens without adhesives). Relatively small COV values (i.e., ≤0.08) of the failure load are observed for the N and N-T specimens, which can be explained by the simple load resistance mechanism of these configurations, with a sole contribution from the ring shank nails through friction. In contrast, increased variability (i.e., $0.09 \leq \text{COV} \leq 0.29$) was observed for specimens with adhesives, which might be attributed to the higher number of factors that affected the load capacity, such as variations in wood grains, the thickness of the adhesive layer, and the failure modes.

The energy dissipation and the ductility ratio values provide some insight into the failure modes of the connections. The N-PU and N-T-PU configurations failed at a larger displacement of 7.4 mm (0.29 in.) and 14.8 mm (0.58 in.), respectively, compared with the N-PE and N-T-PE configurations at 4.7 mm (0.19 in.) and 12.2 mm (0.48 in.), respectively. Therefore, applying polyurethane adhesive in these configurations led to dissipation of a higher amount of energy. However, the lower ductility ratio of this configuration indicates that because of the wood failure mode, a large displacement occurred before the proportional yield limit, as opposed to the polyether configuration with a cohesive failure (i.e., the failure occurred in the adhesive layer). In fact, it can be seen from Table 4 that the ductility ratios of both tied and untied configurations with polyether are higher than those of their respective reference specimens, whereas the polyurethane adhesive decreased the ductility ratios in the connection. With the addition of hurricane ties, the tied specimens showed more ductility and capacities in load and deformation than their counterparts without ties. The initial stiffness values in Table 4 show that the connections with the adhesives were generally three to five times stiffer than the counterpart connections without adhesives.

For easy comparisons, bar charts showing the multiplication factors of the load capacity and energy dissipation of the configurations with adhesives relative to those of their counterpart configurations are presented in Figs. 9(a and c). The results of adding adhesives to the N specimens show that the polyurethane increased the load capacity by about 3.6 times and the polyether by about 4.6 times. As for the addition of the adhesives to the N-T specimens, the load capacity generally doubled. Dissipating energy increased six to seven times for the N-PU and N-PE specimens compared with the N specimens, whereas these values doubled in the tied specimens with adhesives versus without adhesives.

With hurricane ties, the load capacity increased approximately twice, while the energy dissipation increased about 10 times compared with the nail-only configuration [see the left sidebar, Figs. 9(b and d)]. The large increase in energy dissipation mainly resulted from the significantly increased deformation capacities due to the introduction of the ties, which can be seen from Table 4. Similar observations were also made in the many contributions to the literature that investigated the connections' behavior using metal connectors and nails.

The potential alternative of replacing hurricane ties with adhesives in the rafter-to-top-plates connections was also explored by comparing the load capacity and energy dissipation of the N-PE and N-PU specimens with the N-T specimens, as shown in the right two bars in Figs. 9(b and d). This replacement increased the uplift

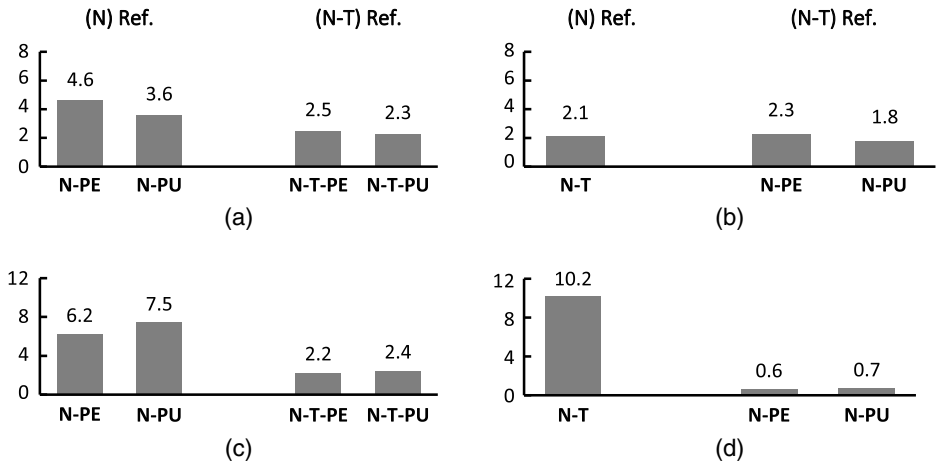

Fig. 9. Multiplication factors to reference specimens: (a and b) load capacity; and (c and d) energy dissipation.

capacity approximately twice but decreased the dissipation energy by approximately 30%–40% owing to the reduced displacements at the failure loads. However, the large deformation capacities of the N-T connections were accompanied by a large gap between the rafter and the top plate at failure. The resulting openings would allow more wind flows through that increase internal pressure and intensify the uplift loading on connections and other components (Simiu and Scanlan 1996).

Conclusions

A new roof-to-wall connection using elastomeric adhesives is proposed to provide an affordable, efficient, and nonintrusive solution for light-frame wood construction. A total of 30 rafter-to-top-plates specimens representing six configurations were fabricated, and their performance to resist the uplift wind load was evaluated through monotonic uplift experiments. The force–displacement curve of each specimen was obtained, and the characteristic parameters were calculated based on the average curve of the six configurations. In addition, failure modes were inspected to provide reasonable explanations for the capacities of each configuration. Test results show that the connections with adhesives increased uplift load capacity by approximately 200%–460%, increased energy dissipation by approximately 200%–750%, and increased initial stiffness by approximately 300%–500% compared with the reference specimens without adhesives. The ductility of connections was improved by the application of polyether as opposed to polyurethane. Replacing hurricane ties in the connections with the adhesives approximately doubled the load capacities and reduced the energy dissipation and deformation capacity.

Besides increasing load capacities, applying adhesives to roof connections causes a considerable reduction in deformation under the same load level, which minimizes the adverse effects associated with water and air intrusion into buildings. The variations in the uplift capacities and failure behaviors using the two adhesives indicate that the roof connections may be designed to achieve a certain performance based on the selection of adhesives. However, before these changes are widely adopted, further research is needed to evaluate fatigue strength, durability behavior, and applicability conditions on the proposed roof connection construction method using adhesives.

Acknowledgments

The authors acknowledge the funding received through Georgeau Construction Research Institute under the project grants program. They also thank Mr. Phillip Georgeau, president of Green Link Institute, for his technical support and selecting the adhesives used in this study. The authors appreciate the help of Emad Zaghalil, graduate student at Western Michigan University, in constructing the test specimens and conducting some of the tests.

References

Alldredge, D. J., J. A. Gilbert, H. A. Toutanji, T. Lavin, and M. S. Balasubramanyam. 2012. "Uplift capacity of polyurea-coated light-frame rafter to top plate connections." *J. Mater. Civ. Eng.* 24 (9): 1201–1210. https://doi.org/10.1061/(ASCE)MT.1943-5533.0000492.

American Wood Council. 2018. *National design specification (NDS)*. Leesburg, VA: American Wood Council.

ASTM. 2012. *Standard test methods for mechanical fasteners in wood*. ASTM D1761. West Conshohocken, PA: ASTM.

ASTM. 2017a. *Standard specification for driven fasteners: Nails, spikes, and staples*. ASTM F1667. West Conshohocken, PA: ASTM.

ASTM. 2017b. *Standard test method for strength properties of adhesives in shear by tension loading*. ASTM D2339. West Conshohocken, PA: ASTM.

ASTM. 2018. *Standard test methods for cyclic (reversed) load test for shear resistance of vertical elements of the lateral force resisting systems for buildings*. ASTM E2126. West Conshohocken, PA: ASTM.

Canbek, C., A. Mirmiran, A. G. Chowdhury, and N. Suksawang. 2011. "Development of fiber-reinforced polymer roof-to-wall connection." *J. Compos. Constr.* 15 (4): 644–652. https://doi.org/10.1061/(ASCE)CC.1943-5614.0000194.

Cheng, J. 2004. "Testing and analysis of the toe-nailed connection in the residential roof-to-wall system." *For. Products J.* 54 (4): 58–65.

Conner, H. W., D. S. Gromala, and D. W. Burgess. 1987. "Roof connections in houses: Key to wind resistance." *J. Struct. Eng.* 113 (12): 2459–2474. https://doi.org/10.1061/(ASCE)0733-9445(1987)113:12(2459).

Datin, P. L., D. O. Prevatt, and W. Pang. 2011. "Wind-uplift capacity of residential wood roof-sheathing panels retrofitted with insulating foam adhesive." *J. Archit. Eng.* 17 (4): 144–154. https://doi.org/10.1061/(ASCE)AE.1943-5568.0000034.

Dias, P. 2015. "Is toughness a better metaphor than resilience ?" *Civ. Eng. Environ. Syst.* 32 (1–2): 68–76. https://doi.org/10.1080/10286608.2015.1016922.

Edmonson, W. C., S. D. Schiff, and B. G. Nielson. 2012. "Behavior of light-framed wood roof-to-wall connectors using aged lumber and multiple connection mechanisms." *J. Perform. Constr. Facil.* 26 (1): 26–37. https://doi.org/10.1061/(ASCE)CF.1943-5509.0000201.

Ellingwood, B. R., D. V. Rosowsky, Y. Li, and J. H. Kim. 2004. "Fragility assessment of light-frame wood construction subjected to wind and earthquake hazards." *J. Struct. Eng.* 130 (12): 1921–1930. https://doi.org/10.1061/(ASCE)0733-9445(2004)130:12(1921).

FEMA. 2006. *Summary report on building performance: Hurricane Katrina 2005*. FEMA 548. Washington, DC: FEMA.

FEMA. 2010. *Home builder's guide to coastal construction: Technical fact sheet series*. Washington, DC: FEMA.

FEMA. 2012. *Spring 2011 tornadoes: Building performance observations, recommendations, and technical guidance: Mitigation Assessment Team report*. Washington, DC: US Dept. of Homeland Security, FEMA.

Forest Products Laboratory. 1952. *Technical note number 119: Strength of southern pine and Douglas-fir compared*. Madison, WI: Forest Products Laboratory.

Forest Products Laboratory. 1978. *Adhesives in building construction*. Madison, WI: Forest Products Laboratory.

Frihart, C. R., and J. F. Beecher. 2016. "Factors that lead to failure with wood adhesive bonds." In *Proc., World Conf. on Timber Engineering*. Washington, DC: United States Dept. of Agriculture.

Gillespie, R. H., and B. H. River. 1972. *Elastomeric adhesive in building construction*, 11–23. Madison, WI: Forest Products Laboratory Forest Service, US Dept. of Agriculture.

Henderson, D. J., J. D. Ginger, M. J. Morrison, and G. A. Kopp. 2009. "Simulated tropical cyclonic winds for low cycle fatigue loading of steel roofing." *Wind Struct.* 12 (4): 383–400. https://doi.org/10.12989/was.2009.12.4.383.

IBHS (Insurance Institute for Business & Home Safety). 2019. *The FORTIFIED HomeTM–Hurricane standard*. Tampa, FL: IBHS.

Jacobs, W. P. V. 2003. *Performance of pressure sensitive adhesive tapes in wood light-frame shear walls*. Blacksburg, VA: Univ. Libraries, Virginia Polytechnic Institute and State Univ.

Loushin, S. 2012. "Choosing and using structural adhesives." Accessed November 14, 2018. http://www.machinedesign.com/adhesives/choosing-and-using-structural-adhesives.

Muñoz, W., A. Salenikovich, M. Mohammad, and P. Quenneville. 2008. *Determination of yield point and ductility of timber assemblies: In search for a harmonised approach*. Madison, WI: Wood Products Association.

NOAA (National Oceanic and Atmospheric Administration). 2017. "U.S. billion-dollar weather and climate disasters 1980-2017." Accessed January 14, 2018. https://www.ncdc.noaa.gov/billions/.

Rammer, D. R., S. G. Winistorfer, and D. A. Bender. 2001. "Withdrawal strength of threaded nails." *J. Struct. Eng.* 127 (4): 442–449. https://doi.org/10.1061/(ASCE)0733-9445(2001)127:4(442).

Reed, T. D., D. V. Rosowsky, and S. D. Schiff. 1997. "Uplift capacity of light-frame rafter to top plate connections." *J. Archit. Eng.* 3 (4): 156–163. https://doi.org/10.1061/(ASCE)1076-0431(1997)3:4(156).

Rosowsky, D. V., T. D. Reed, K. G. Tyner, and R. Rosowsky. 1998. "Establishing uplift design values for metal connectors in light-frame construction." *J. Test. Eval.* 26 (5): 426–433. https://doi.org/10.1520/JTE12024J.

Satheeskumar, N., D. J. Henderson, J. D. Ginger, and C. H. Wang. 2016. "Wind uplift strength capacity variation in roof-to-wall connections of timber-framed houses." *J. Archit. Eng.* 22 (2): 04016003. https://doi.org/10.1061/(ASCE)AE.1943-5568.0000204.

Shanmugam, B., B. G. Nielson, and S. D. Schiff. 2011. "Multi-axis treatment of typical light-frame wood roof-to-wall metal connectors in design." *Eng. Struct.* 33 (12): 3125–3135. https://doi.org/10.1016/j.engstruct.2011.07.031.

Simiu, E., and R. H. Scanlan. 1996. *Wind effects on structures: Fundamentals and applications to design*. 3rd ed. Mineola, NY: Dover Publications.

Simpson Strong Ties. 2019. "Wood construction connectors Catalog." Accessed April 24, 2019. https://embed.widencdn.net/pdf/plus/ssttoolbox/jg8ztjcq8z/C-C-2019.pdf.

Tse, M. F. 1989. "Studies of triblock copolymer-tackifying resin interactions by viscoelasticity and adhesive performance." *J. Adhes. Sci. Technol.* 3 (1): 551–570. https://doi.org/10.1163/156856189X00407.

Turner, M. A., R. H. Plaut, D. A. Dillard, J. R. Loferski, and R. Caudill. 2009. "Tests of adhesives to augment nails in wind uplift resistance of roofs." *J. Struct. Eng.* 135 (1): 88–93. https://doi.org/10.1061/(ASCE)0733-9445(2009)135:1(88).